

# Simulation of Electroosmosis Using a Meshless Finite Point Method

M.J. Mitchell and N.R. Aluru

University of Illinois, 3263 Beckman Institute MC-251  
405 N. Mathews Ave., Urbana, IL 61801, US

[mjmitch@uiuc.edu](mailto:mjmitch@uiuc.edu), [aluru@uiuc.edu](mailto:aluru@uiuc.edu)

## ABSTRACT

A Finite Point Method (FPM) based on a weighted least squares interpolation is presented for the simulation of electroosmotic transport in capillaries. This method requires no mesh and involves no Galerkin-type integration, making it more computationally efficient than the traditional finite element method.

The FPM has been employed to solve the non-linear Poisson-Boltzmann equation for charge distribution, the Laplace equation for applied potential, and the Stokes equations for fluidic transport. These equations govern electroosmotic transport, the phenomenon used to drive fluid through electrophoretic separation systems.

**Keywords:** meshless methods, electroosmosis, MEMS

## INTRODUCTION

An emerging technology in the area of biological micro-electromechanical systems (BioMEMS) is the electrophoretic separation of fluid components in micro total analysis systems ( $\mu$ TAS). This procedure is carried out in capillary channels that have been integrated onto microchips. Cost-effective design and fabrication of these devices requires computationally efficient simulation tools. Currently, these tools use mesh-based methods such as the finite element and finite difference methods to solve the governing differential equations [1,3].

In this paper we present a truly meshless FPM based on quadratic interpolation functions and apply it to electroosmosis. The method, originally introduced by Oñate et. al. [4] and extended here to simulate electroosmosis, requires that the domain be defined only by point distribution with no connectivity information required. The method also requires no background grid, making it truly meshless.

The new method has been applied to the equations governing electroosmosis in two geometries, a straight channel and a cross-shaped channel intersection. Analytical solutions for the straight channel have been published by Patankar and Hu [1] and reproduced by our code. Patankar and Hu have also modeled the electroosmotic phenomenon in a cross-shaped channel. Results from two dimensional simulations of the same geometry are presented and compared to those published in [1].

## PROBLEM FORMULATION

The equations governing the distribution of charge in the electric double layer near a solution-capillary interface and the resulting fluid motion due to an applied potential difference are well-known [2,3,5,6,7]. Under the assumption that the zeta potential effects extend only a small distance into the channel, the applied potential gradients can be assumed to have no effect on the charge distribution near the walls [7]. Therefore, we can separate the two potentials in the formulation of the problem.

The  $\zeta$ -potential at the solution-capillary interface result in a  $\Psi$ -field. The corresponding charge density, assuming a symmetric salt, is given by

$$\rho_E = -2zFc_0 \sinh\left(\frac{zF\Psi}{RT}\right) \quad (1)$$

where  $\rho_E$  is the charge density  $z$  is the charge number of the ions  $F$  is Faraday's constant,  $c_0$  is the ionic concentration in the solution bulk,  $R$  is the gas constant, and  $T$  is the temperature. Combining equation (1) and Poisson's equation relating charge and potential, we obtain the Poisson-Boltzmann equation

$$\nabla^2\Psi = \frac{2zFc_0}{\epsilon} \sinh\left(\frac{zF\Psi}{RT}\right) \quad (2)$$

where  $\epsilon$  denotes the electric permittivity of the normal aqueous solution.

The potentials applied at the ends of the channel result in a  $\Phi$ -field whose distribution can be determined by solving the Laplacian

$$\nabla^2\Phi = 0 \quad (3)$$

The final equation governing the transport of the fluid subjected to an electric field is given by the Stokes equations for incompressible steady flow

$$\begin{aligned} \mu\nabla^2\vec{u} - \nabla p &= -\rho_E\vec{E} \\ \nabla \cdot \vec{u} &= 0 \end{aligned} \quad (4)$$

where  $\mu$  is the viscosity of the fluid,  $\vec{u}$  is the velocity vector,  $p$  is the pressure, and the electric field intensity is given by  $\vec{E} = -\nabla\Phi$ . By substituting expressions for the charge concentration (1) and electric field intensity, the Stokes equations can be rewritten as

$$\mu\nabla^2\vec{u} - \nabla p = -\frac{2zFc_0}{\epsilon} \sinh(\Psi)(\nabla \cdot \Phi) \quad (5)$$

$$\nabla \cdot \vec{u} = 0$$

For numerical solution, the equations governing electroosmotic transport (2,3,5) were formulated in dimensionless variables in the style of Harrison et. al. [3].

## FINITE POINT METHOD

The FPM employed to solve the equations governing electroosmotic transport is based on the method introduced by Oñate et. al. [4]. This method minimizes the weighted squared approximation error at each node in the domain, expressed by the function

$$J = \sum_{j=1}^n \varphi(x_j)(u_j^h - \bar{p}^T \bar{\alpha})^2 \quad (6)$$

where  $\varphi$  is a weighting function whose value is non-zero at  $n$  nodes and whose domain of influence is termed a cloud.  $u_j^h$  represents the exact nodal values,  $\bar{p}^T$  is a vector of monomials that define the basis functions, and  $\bar{\alpha}$  is a vector of interpolation coefficients. For two-dimensional analysis, the weighting function is defined as a tensor product of two orthogonal one-dimensional Gaussian functions. For a two-dimensional quadratic interpolation, the vector of monomials and the corresponding interpolation coefficients are given by

$$\bar{p}^T = [1 \quad x \quad y \quad x^2 \quad xy \quad y^2] \quad (7)$$

$$\bar{\alpha}_j^T = [\alpha_0^j \quad \alpha_1^j \quad \alpha_2^j \quad \alpha_3^j \quad \alpha_4^j \quad \alpha_5^j]$$

For a given weighting function, the quantity  $J$  is minimized with respect to  $\bar{\alpha}$ , resulting in a local expression for  $\bar{\alpha}$ .

$$\bar{\alpha} = \bar{C}^{-1} \bar{u}^h \quad (8)$$

where

$$\bar{C}^{-1} = A^{-1}B \quad (9)$$

with matrices  $A$  and  $B$  given by

$$A = \sum_{j=1}^n \varphi(\bar{x}_j) \bar{p}(\bar{x}_j) \bar{p}^T(\bar{x}_j) \quad (10)$$

$$B = [\varphi(\bar{x}_1) \bar{p}(\bar{x}_1) \quad \varphi(\bar{x}_2) \bar{p}(\bar{x}_2) \quad \dots \quad \varphi(\bar{x}_3) \bar{p}(\bar{x}_3)]$$

The local basis functions are then constructed by

$$N_j(\bar{x}) = \bar{p}^T(\bar{x}) \bar{C}^{-1} \quad (11)$$

Because the weighting function is fixed for a given cloud, the  $\bar{C}^{-1}$  matrix is constant over the entire cloud. Therefore, the derivatives of the basis functions are given by

$$\frac{\partial N_j(\bar{x})}{\partial x} = \frac{\partial \bar{p}^T(\bar{x})}{\partial x} \bar{C}^{-1} \quad (12)$$

where

$$\frac{\partial \bar{p}^T(\bar{x})}{\partial x} = [0 \quad 1 \quad 0 \quad 2x \quad y \quad 0] \quad (13)$$

The global basis function matrices are obtained by placing a weighting function at each point in the domain and performing these calculations for each cloud. The approximation to the function can now be expressed as

$$u(\bar{x}_j) \cong \hat{u}(\bar{x}_j) = \sum_{A=1}^n N_A(\bar{x}_j) u_A \quad (14)$$

where  $N_A$  denotes the value of the basis function centered at  $\bar{x}_A$  evaluated at  $\bar{x}_j$  and  $u_A$  denotes the nodal parameters. Due to the least squares nature of the formulation, it should be noted that  $u_A$  and  $u(\bar{x}_A)$  will typically not have the same value.

This method has been employed in the solution of the governing equations of electroosmotic transport. The non-linear Poisson-Boltzmann equation has been solved for  $\Psi$  using a Newton iteration algorithm.  $\Psi$  has been prescribed to the  $\zeta$ -potential on the walls, with a developed field enforced at the reservoirs. The Laplacian of  $\Phi$  has been solved with prescribed values at the reservoirs and an insulation condition at the walls. Finally, a stabilized formulation of the Stokes equations has been solved with no-slip velocity conditions and Neumann pressure conditions on the walls, as well as developed velocity fields and prescribed pressures at the reservoirs.

## RESULTS

The FPM was tested extensively on algebraic patch tests and then employed for simulating steady Stokes flow. After matching our results with analytical solutions for these problems, the method was then extended to simulate electroosmosis. In a straight channel the governing equations essentially reduce to a one-dimensional problem. The geometry and parameter values are shown in Figure 1. A very narrow channel has been chosen to allow us to see the variations in  $\Psi$  and the corresponding velocities near the walls. Profile plots of the  $\Psi$  component of potential and  $x$  component of velocity at the center of the channel are shown in Figure 2 and Figure 3, respectively, along with the analytical results presented in [1].

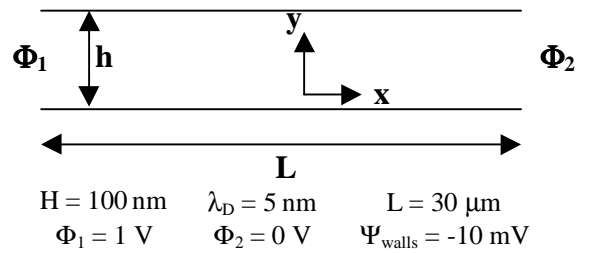


Figure 1

The potential and velocity both assume their characteristically flat profiles in the center of the channel. Also, notice that the negative surface potential leads to an accumulation of positive charge near the surface. This charge, when acted on by a positive electric field, results in left to right flow, or positive velocity.

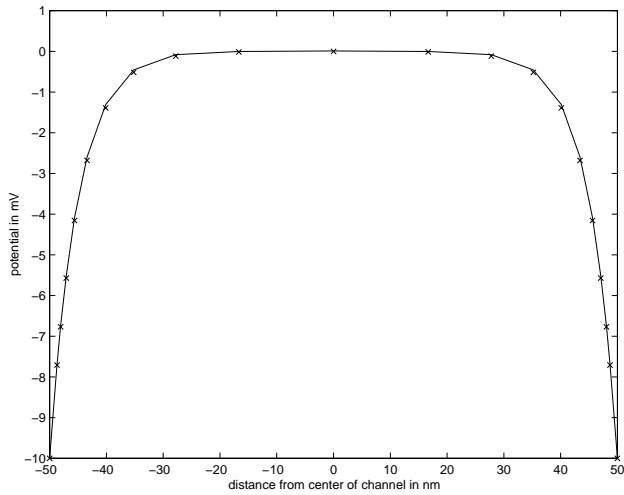


Figure 2 : Profile of potential due to  $\zeta$ -potential. Analytical values are represented by x's

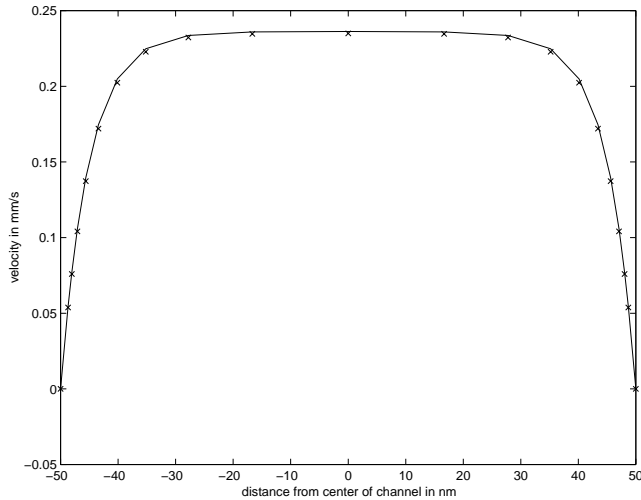


Figure 3 : Velocity profile in straight channel. Analytical values are represented by x's

The next device that we have simulated is a cross-shaped channel as shown in Figure 4[1]. Results for this problem are presented in dimensionless quantities. The non-uniform point distribution used near the intersection is shown in Figure 5. Contour plots of the applied potential for two cases of applied side reservoir potential and the corresponding velocity vector plots are shown in Figure 6 and Figure 7, respectively.

A denser point distribution is used in the vicinity of the walls because significant gradients in potentials and velocities occur within the finite double layer. The width of this layer has been chosen large for this problem as well so that we can see the variation in potential and velocity near the walls.

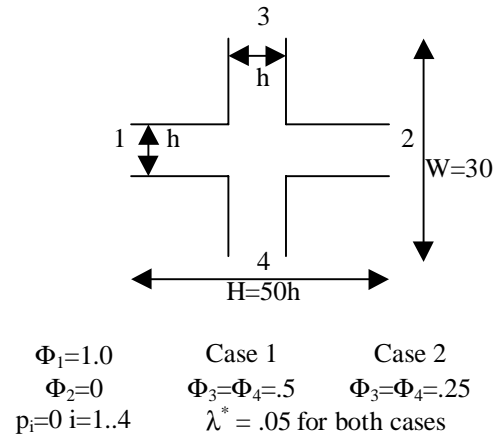


Figure 4 : Geometry of cross-channel

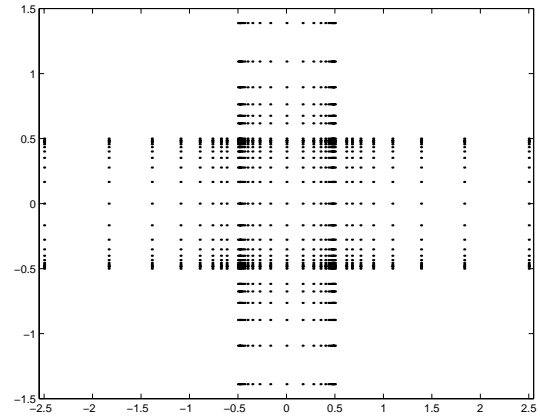


Figure 5 : Point distribution near intersection

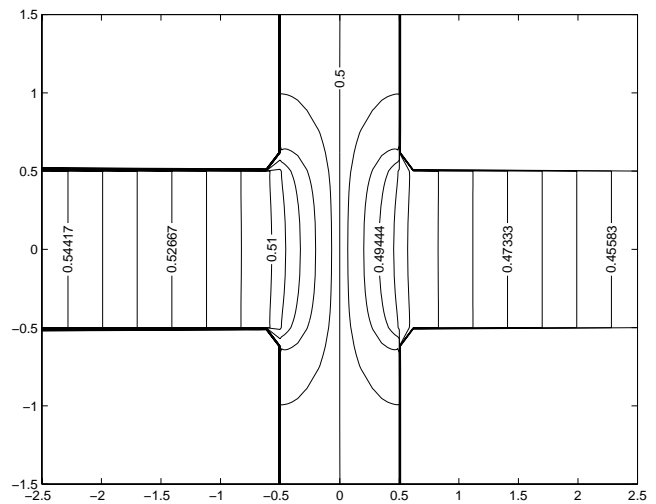


Figure 6a: Applied potential contours near intersection for symmetric case with side reservoirs held at  $\Phi=.5$

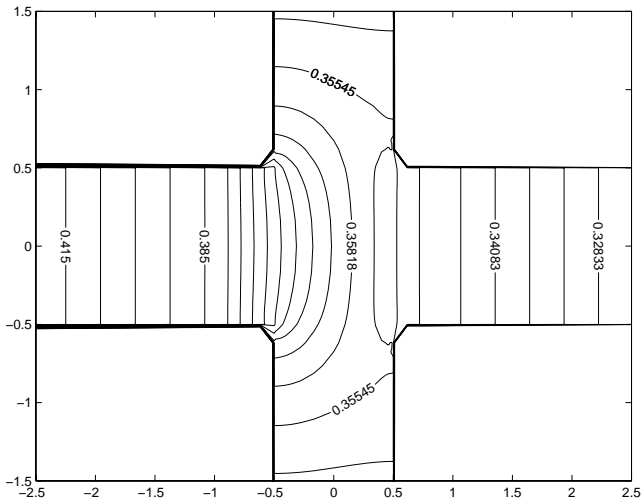


Figure 6b: Applied potential contours for non-symmetric case with side reservoirs held at  $\Phi=.25$

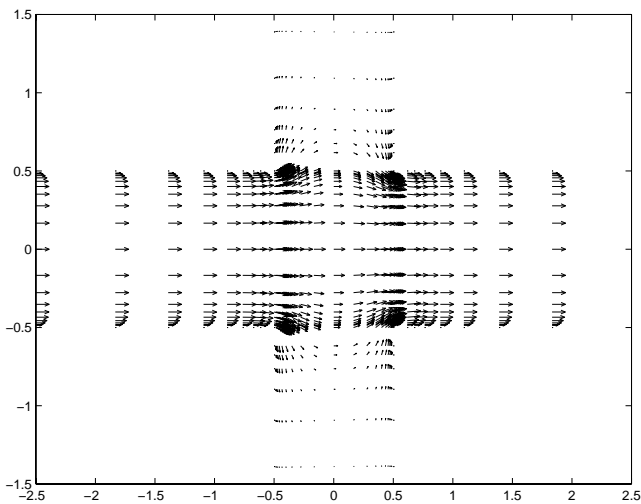


Figure 7a : Velocity vectors for symmetric applied potential

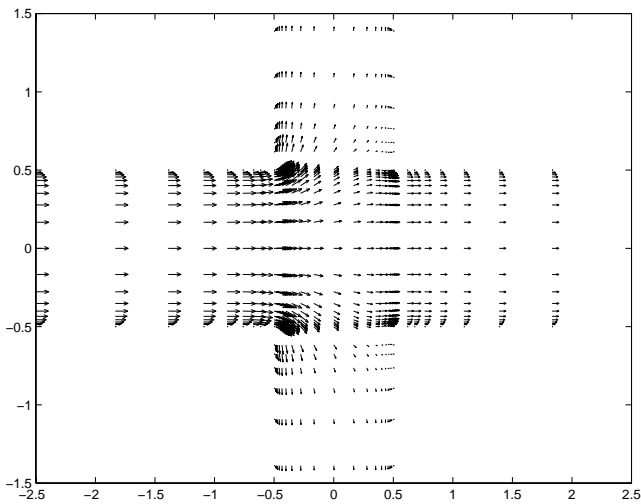


Figure 7b : Velocity vectors for non-symmetric potential

For the symmetric case, a constant potential line of .5 exists across the middle of the side channels and the intersection. As a result, no net flow occurs at the side reservoirs. Instead, the fluid that flows into the side channels returns to the main channel, resulting in a negligible decrease in main channel velocity across the intersection. For the non-symmetric case, however, gradients in the potential are observed in the side channels, resulting in significant leakage into reservoirs 3 and 4.

## CONCLUSION

A new Finite Point Method has been presented for the simulation of electroosmosis. A weighted least squares interpolation scheme has been used to derive shape functions. A point collocation method is then employed to satisfy the governing equations at each point. Each of the three sets of equations that together govern electroosmosis has been solved by this method.

The new method has matched analytical results for a straight channel and qualitatively matched published results for a cross-shaped channel [1]. The advantage of this method over other PDE solvers is the computational savings due to a lack of mesh generation and integration. For this reason, the FPM can be used to make more efficient simulation tools for MEMS design.

## ACKNOWLEDGMENT

This work is supported by a grant from the DARPA Composite CAD Program, Air Force Research Laboratory, Air Force Material Command under agreement number F30602-98-2-0178.

## REFERENCES

- [1] Patankar and Hu, Anal. Chem. 70, 1870-1881, 1998.
- [2] Probst, "Physicochemical Hydrodynamics," Wiley & Sons, 190-202, 1994.
- [3] Harrison, et. al., Transducers 1997, 923-926.
- [4] Oñate, et. al., Comp. Meth. Appl. Mech. Engrg. 139, 315-346, 1996.
- [5] Molho et. al., ASME-DSC-66 1998, 69-76
- [6] Rice and Whitehead, J. Phys. Chem., 69, 4017-4024, 1965.
- [7] Deshpande, et. al., SPIE Vol. 3515, 217-227, 1998.